DOI: 10.1002/chem.200501515

A Three-State Model for the Photophysics of Adenine

Luis Serrano-Andrés,*[a] Manuela Merchán,[a] and Antonio Carlos Borin[b]

Abstract: An ab initio theoretical study at the CASPT2 level is reported on minimum energy reaction paths, state minima, transition states, reaction barriers, and conical intersections on the potential energy hypersurfaces of two tautomers of adenine: 9*H*- and 7*H*-adenine. The obtained results led to a complete interpretation of the photophysics of adenine and derivatives, both under jet-cooled conditions and in solution, within a three-state model. The ultrafast subpicosecond fluorescence decay measured in adenine is attributed to the low-lying conical intersection $(gs/\pi\pi^* L_a)_{CI}$, reached from the initially populated $^1(\pi\pi^* L_a)$ state along a path which is found to be barrierless only in 9*H*-adenine, while for the 7*H* tautomer the presence of an intermediate plateau corresponding to an NH_2-twisted conformation may explain the absence of ultrafast decay in 7-substituted compounds. A secondary picosecond decay is assigned to a path involving switches towards two other states, $^1(\pi\pi^* L_b)$ and $^1(n\pi^*)$, ultimately leading to another conical intersection with the ground state, $(gs/n\pi^*)$, with a perpendicular disposition of the amino group. The topology of the hypersurfaces and the state properties explain the absence of secondary decay in 9-substituted adenines in water in terms of the higher position of the $^1(n\pi^*)$ state and also that the $^1(\pi\pi^* L_b)$ state of 7*H*-adenine is responsible for the observed fluorescence in water. A detailed discussion comparing recent experimental and theoretical findings is given. As for other nucleobases, the predominant role of a $\pi\pi^*$-type state in the ultrafast deactivation of adenine is confirmed.

Keywords: ab initio calculations · adenine · nucleobases · photochemistry · photophysics

Introduction

Photostability is the primary photophysical property attributed to DNA and RNA after interaction with UV light, a quality probably acquired after a long period of natural evolution.[1] Early measurements on nucleobase monomers in aqueous phase provided low fluorescence quantum yields[2–7] and indirect evidence of extremely efficient nonradiative decay to nonemitting states.[5–8] Recently, however, ultrafast internal conversion events in nucleic acids were directly detected by subpicosecond techniques as a common feature of nucleotides, nucleosides, and nucleobase monomers, under isolated conditions, in condensed phases, or integrated in polynucleotide chains.[19–12] To understand the relaxation pathways of electronically excited nucleic acid molecules is probably one of the most important challenges in current photobiology, in particular to determine mechanisms of DNA and RNA damage and repair, to understand energy- and charge-transfer processes in polynucleotides, and to monitor intrinsic fluorescence in regular nucleobases or derivatives as a probe of DNA molecular dynamics.[1,8] Although many other deactivation mechanisms may be available in single- and double-stranded nucleic acids, it is of primary interest to determine the intrinsic decay pathways associated with the base monomers. Nowadays, such a task cannot be undertaken without the contribution of highly accurate multiconfigurational ab initio quantum-chemical methods able to identify decay funnels, as proved by the join efforts of different groups over the last few years to merge complementary theoretical and experimental findings.[1,13–23]

The quantum-chemical vision of a photoinduced process is based on the topology of the ground- and excited-state potential energy surfaces (PES), the minimum-energy reaction paths connecting different regions of the PES where the energy evolves after absorption of energy, and the location and accessibility of the minima and conical intersec-

[a] Dr. L. Serrano-Andrés, Prof. M. Merchán
Instituto de Ciencia Molecular
Universitat de València
Dr. Moliner 50, Burjassot, 46100 Valencia (Spain)
Fax: (+34) 96-354-3156
E-mail: Luis.Serrano@uv.es

[b] Dr. A. C. Borin
Instituto de Química, Universidade de São Paulo
Av. Prof. Lineu Prestes 748, 05508–900, São Paulo, SP (Brazil)

Supporting information for this article is available on the WWW under http://www.chemeurj.org/ or from the author.

tions, whereby the former are responsible for slow emission processes, and the latter for rapid nonradiative decays.[24–28] The information required to understand or predict the photophysics of the molecules includes accurate determination of reaction paths, energy barriers to surmount in order to escape from minima and access conical intersections, and the properties of the related excited states and transitions, such as dipole moments and transition probabilities. Time-resolved measurements on DNA/RNA nucleobases (adenine, guanine, cytosine, thymine, and uracil) seem to indicate a common set of mechanisms related to their internal conversion processes.[1] In particular, the most recent analysis of the data in molecular beams excited at 267 nm (4.64 eV) strongly supports double-exponential energy decays, one with a short relaxation lifetime near 100–160 fs and a second, long-lived relaxation around 1.1–5.1 ps,[10] also present, with small variations, in condensed phases, and for nucleosides and nucleotides.[1,11] The strong dependence of the conclusions on the experimental conditions and the selected exponential fitting makes it difficult to obtain a clear view of the problem, which requires studies at higher resolution that also elucidate the role of tautomers. Adenine is the most studied molecule from an experimental standpoint, although the contribution of at least two close-energy tautomers complicates the interpretation of the data.[1,10,11,15,29–32]

Here we report on determining the main internal conversion channels in adenine. As two tautomers of the molecule, 9*H*- and 7*H*-adenine (Figure 1), are so close in energy that they are both considered to contribute to the photophysics, not only in solution but at temperatures needed to vaporize the compound,[1,7,31–35] we included them both in the study, although 7-substituted compounds have secondary biological importance. Calculations involved the PES of the low-lying excited molecular states of the systems at the CASPT2 level, described the main relaxation pathways, and located the most accessible conical intersections. Adenine is one of the most scrutinized nucleobase monomers, and plenty of information about its dynamics of deactivation is also available for its nucleoside, nucleotide, and several derivatives.[1] Two recent and valuable theoretical studies[21,22] located some of the crucial conical intersections for 9*H*-adenine. The present minimum-energy paths, which proved to be essential, profiles, energy barriers, and conical intersections will be used to rationalize the photophysics of both tautomers on the basis of their relaxation pathways from the initially excited singlet state, and the results will help us to interpret the available experimental data of adenine and different derivatives measured in different environments. Once more,[7,17,20–22] the predominant role of a ππ*-type state in the ultrafast deactivation of nucleic acid nucleobases is outlined.

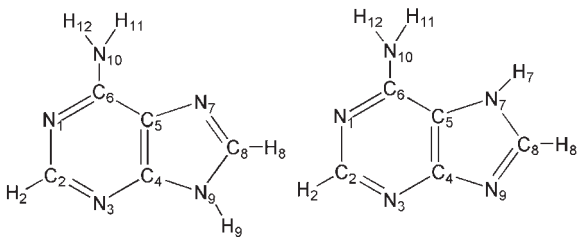

Figure 1. Structure and atom labeling for 9*H*-adenine (left) and 7*H*-adenine (right).

Computational Details

Optimizations of minima, transition states, PES crossings, and minimum-energy reaction paths (MEPs), as implemented in the MOLCAS package, were performed initially at the CASSCF level of theory for both the 9*H* and 7*H* tautomers of adenine. MEPs were built as steepest descendent paths in which each step requires minimization of the PES on a hyperspherical cross section of the PES centered on the initial geometry and characterized by a predefined radius (see Supporting Information). At the computed points, CASPT2 calculations on several singlet states were carried out in order to include the necessary dynamic correlation effects. The protocol is usually named CASPT2//CASSCF, and has proved its accuracy repeatedly.[17,18,23,27,36–40] At the obtained CASSCF crossings, CASPT2 scans at close geometries were performed to find lowest energy CASPT2 crossings pointing to conical intersections at the highest level of calculation. The one-electron atomic basis set 6-31G(d,p) was used throughout for energy optimizations and energy differences, in order to obtain a balanced description of the PES. The minor influence of diffuse functions to describe low-lying valence excited states of adenine was shown previously.[41] The accuracy of the present strategy regarding the use of larger basis sets can be compared to our previous study on adenine in which large ANO-type basis sets were employed.[37,42] Unless otherwise specified (see also Supporting Information), the final results use an active space of 11 orbitals and 12 electrons. No symmetry restrictions were imposed during the calculations, which employed in all cases the MOLCAS-6 set of programs.[43] From the calculated CASSCF transition dipole moments (TDM) and the CASPT2 band origin energies, the radiative lifetimes were estimated by using the Strickler–Berg relationship.[27,44,45] Additional technical details can be found in the Supporting Information, in particular the CASSCF reaction paths and the Cartesian coordinates of the described geometries.

Results and Discussion

Potential energy hypersurfaces of 9*H*-adenine and 7*H*-adenine: The description of adenine photophysics starts with the structure and properties of the low-lying singlet excited states at the ground-state geometry of the molecule, the so-called Franck–Condon (FC) region. Tables 1 and 2 compile the computed absorption and emission energies, oscillator strengths, dipole moments, and radiative lifetimes for the low-lying singlet states of 9*H*-adenine and 7*H*-adenine. In both tautomers, the singlet states follow the vertical order nπ*, ππ* L_b, and ππ* L_a at the CASPT2 level. Platt's nomenclature[46] allows us to distinguish between the two low-lying ππ* states: ^{1}(ππ* L_a) can be described mainly by the HOMO (H)→LUMO (L) transition, and ^{1}(ππ* L_b) by a linear combination of configurations H→L+1 and H−1→L. On the other hand, the lowest ^{1}(nπ*) state involves transitions from the nitrogen atoms at the pyrimidine ring towards the π structure. Considering the values of the oscillator strengths of the the ^{1}(ππ* L_a) transitions (0.1747 and 0.0723 for 9*H*- and 7*H*-adenine, respectively), it is deter-

Table 1. Computed spectroscopic properties for the low-lying singlet excited states of 9*H*-adenine at the CASPT2//CASSCF(16,13)/6-31G(d,p) level.

State	Vertical absorption [eV] CASSCF	CASPT2	μ(D)	Band origin (T_e [eV])[a] CASSCF	CASPT2	τ_{rad} (ns)[b]
^{1}(gs)			2.67			
^{1}(nπ*)	5.95	4.96 (0.0037)	1.99	4.88	4.52	334
^{1}(ππ* L_b)	5.56	5.16 (0.0042)	2.46	4.92	4.83	251
^{1}(ππ* L_a)[c]	7.03	5.35 (0.1747)	4.17			

[a] Experimental jet-cooled adenine, assigned to 9*H*-adenine: $T_0=4.40$ eV (nπ*) and 4.48 eV (ππ*).[31–34] [b] Fluorescence in water (probably from the ^{1}(ππ* L_b) state of 7*H*-adenine): $T_0=4.43$ eV, $\phi_F=2.6\times10^{-4}$, $\tau_F=8.8$ ps, $\tau_{rad}=\tau_F/\phi_F=34$ ns.[6,59] [c] Geometry optimization leads directly to (gs/ππ* L_a)$_{CI}$.

Table 2. Computed spectroscopic properties for the low-lying singlet excited states of 7*H*-adenine at the CASPT2//CASSCF(16,13)/6-31G(d,p) level.

State	Vertical absorption [eV] CASSCF	CASPT2	μ(D)	Band origin (T_e [eV])[a] CASSCF	CASPT2	τ_{rad} (ns)[b]
^{1}(gs)			6.35			
^{1}(nπ*)	5.59	4.74 (0.0087)	4.14	4.70	4.14	177
^{1}(ππ* L_b)	5.48	5.06 (0.0223)	5.38	4.99	4.60	54
^{1}(ππ* L_a)[c]	7.10	5.41 (0.0723)	8.38			

[a] Experimental jet-cooled adenine: proposed as 7*H*-adenine, $T_0=4.44$ eV (ππ*).[33] [b] Fluorescence in water (probably from the ^{1}(ππ* L_b) state of 7*H*-adenine): $T_0=4.43$ eV, $\phi_F=2.6\times10^{-4}$, $\tau_F=8.8$ ps, $\tau_{rad}=\tau_F/\phi_F=34$ ns.[6,59] [c] Geometry optimization leads directly to (gs/ππ* L_a)$_{CI}$, although a planar local minimum exists at high energy.

mined to carry most of the intensity in both tautomers, and the corresponding state can be denoted as the spectroscopic state. The results are basically coincident with previous CASPT2 studies using more accurate ANO basis sets, except for the absence of low-lying nπ* states in the latter due to limitations in the multiconfigurational description.[42] There is also a slight discrepancy with recent calculations on the vertical spectrum of 9*H*-adenine at the CASPT2//MP2/6-31G(d,p) level[22] with respect to the position of the lowest ^{1}(nπ*) state, placed here at 4.96 eV and reported earlier at 5.50 eV, as the third singlet excited state, while the remaining properties such as oscillator strengths and dipole moments agree in both studies. To check the effect of the geometry we used the MP2/6-31G(d,p) ground-state structure, and the state ordering remained almost as in Table 1: 4.99, 4.97, and 5.28 eV for the ^{1}(nπ*), ^{1}(ππ* L_b), and ^{1}(ππ* L_a) states, respectively. The source of the discrepancy is unknown, probably a problem in the selection of the active space in the previous study.[22] Our results also agree in finding a low-lying ^{1}(nπ*) state with recently reported DFT/MRCI calculations.[21] For a more detailed discussion on the properties of the full UV/Vis absorption spectra of adenine, the reader is referred to the previous CASPT2 analysis.[42]

A proper description of the photochemical processes taking place in molecules must necessarily follow the main path of the energy, in this case starting from the FC absorption and evolving along an MEP related to the spectroscopic state ^{1}(ππ* L_a). Such analysis, based on minimal potential energy profiles, provides a basic mapping of the reaction pathways which will have to be complemented in future with more extended calculations on larger regions of the PES and by including the dynamic aspects of the problem, in order to fully predict the evolution and timescale of the photochemical process. Figure 2 displays the energies of the low-lying singlet excited states of

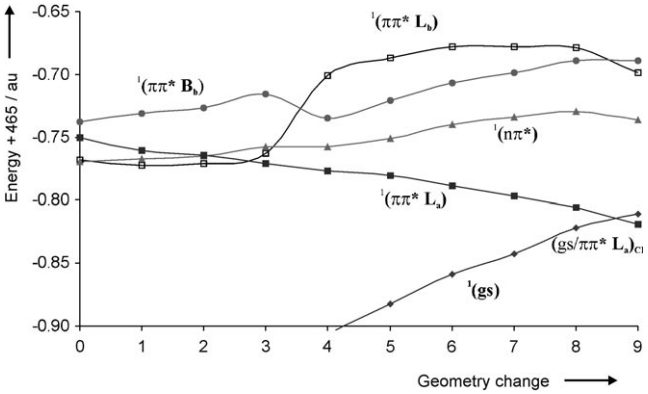

Figure 2. Low-lying singlet excited states of 9*H*-adenine computed at the CASPT2//CASSCF level from the FC ground-state geometry along the MEP on the ^{1}(ππ* L_a) state.

9*H*-adenine computed at the CASPT2 level from the FC ground-state geometry along the CASSCF MEP on the ^{1}(ππ* L_a) hypersurface. The obtained path, after crossing the ^{1}(nπ*) and ^{1}(ππ* L_b) states, leads directly to a conical intersection with the ground state, (gs/ππ* L_a)$_{CI}$. The path has a steepest descendent nature and consequently the ^{1}(ππ* L_a) state has no minimum. As discussed below, this feature is the cornerstone of adenine photochemistry. Considering that on light irradiation the ^{1}(ππ* L_a) state has the major population, the energy will be deactivated to the ground state through the conical intersection (gs/ππ* L_a)$_{CI}$ in an efficient, ultrafast, nonradiative internal conversion process that quenches most of the fluorescence. The ^{1}(nπ*) and ^{1}(ππ* L_b) states will be partially populated just by direct absorption or through the conical intersections found along the ^{1}(ππ* L_a) MEP, that is, (ππ* L_a/nπ*)$_{CI}$ and (ππ* L_a/ππ* L_b)$_{CI}$. Starting at these conical intersections, two MEPs have been computed on the ^{1}(nπ*) and ^{1}(ππ* L_b) state hypersurfaces, respectively, leading to their own energy minima, ^{1}(nπ*)$_{min}$ and ^{1}(ππ* L_b)$_{min}$. These structures are essentially coincident with the CASSCF optimized geometries for the ^{1}(nπ*) and ^{1}(ππ* L_b) states, and both belong to the S_1 hypersurface at all levels of theory, that is, they are the lowest excited state at their respective geometries. These MEPs, computed at the CASPT2 level, are displayed for 9*H*-adenine in

Figures 3 and 4, and represent the relaxation paths on the $^1(\pi\pi^*\ L_b)$ and $^1(n\pi^*)$ states after crossing with the deactivation path of the initially excited spectroscopic $^1(\pi\pi^*\ L_a)$ state.

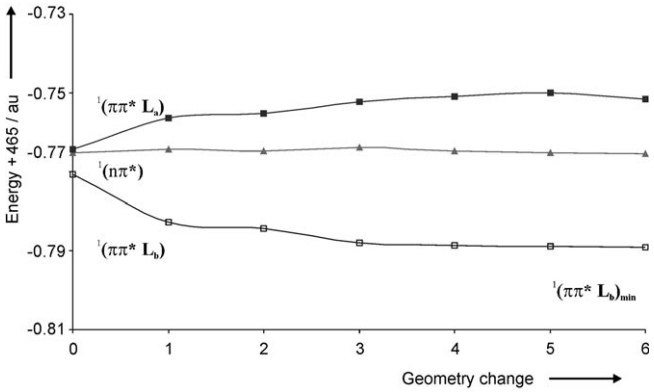

Figure 3. Low-lying singlet excited states of 9*H*-adenine computed at the CASPT2//CASSCF level from the geometry of the $^1(\pi\pi^*\ L_a)/^1(\pi\pi^*\ L_b)$ crossing and along the MEP on the $^1(\pi\pi^*\ L_b)$ state.

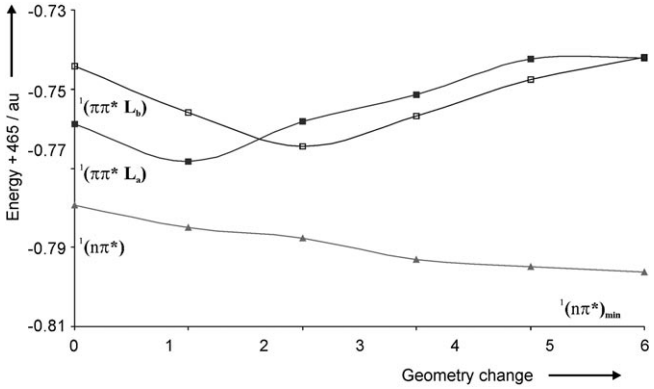

Figure 4. Low-lying singlet excited states of 9*H*-adenine computed at the CASPT2//CASSCF level from the geometry of the $^1(\pi\pi^*\ L_a)/^1(n\pi^*)$ crossing and along the MEP on the $^1(n\pi^*)$ state.

The same strategy was employed for 7*H*-adenine. Figure 5 shows the CASPT2 MEP of its $^1(\pi\pi^*\ L_a)$ excited state starting at the FC region. Surprisingly, the computed path leads to a totally different region than that found for 9*H*-adenine, reaching a structure which is a local minimum on the $^1(\pi\pi^*\ L_a)$ hypersurface that we have coined $^1(\pi\pi^*\ L_a\ NH_2)_{min}$, which has a planar geometry with the NH_2 hydrogen atoms twisted by about 60° and the amino nitrogen lone-pair electrons facing H_7. The character of the state remains, however, the same, that is, $\pi\pi^*$ excitation is restricted to the rings without charge transfer from the NH_2 moiety. As can be noted in Figure 5, the PES around the region of the $^1(\pi\pi^*\ L_a\ NH_2)_{min}$ minimum is quite flat for the three computed singlet excited states, which become almost degenerate and cross at energies similar to those computed for 9*H*-adenine. From those crossings, one can expect that part of the energy

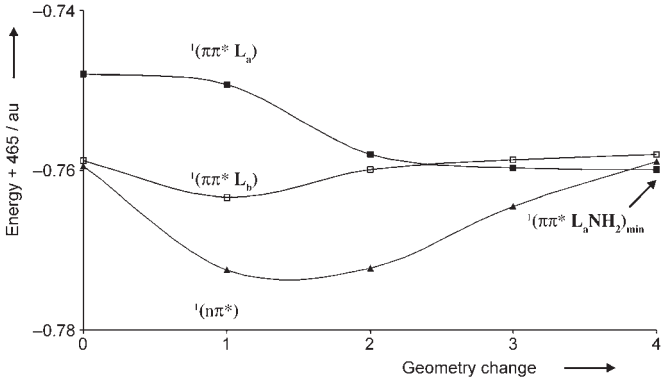

Figure 5. Low-lying singlet excited states of 7*H*-adenine computed at the CASPT2//CASSCF level from the FC ground-state geometry to the geometry of the local minimum $^1(\pi\pi^*\ L_a\ NH_2)_{min}$ along the MEP on the $^1(\pi\pi^*\ L_a)$ state.

can reach the minima of the $^1(n\pi^*)$ and $^1(\pi\pi^*\ L_b)$ states along their respective paths. The $^1(\pi\pi^*\ L_a)$ excited state at this local minimum, $^1(\pi\pi^*\ L_a\ NH_2)_{min}$, located adiabatically at 5.13 eV with respect to the ground-state minimum, becomes the lowest singlet excited state (S_1), will continue to decrease in energy, and, after surmounting the corresponding barrier, will lead to the same conical intersection as that found for the 9*H* tautomer, that is, $(gs/\pi\pi^*\ L_a)_{CI}$, in a barrierless way. The corresponding CASPT2 path for 7*H*-adenine is included in the Supporting Information.

The topologies of the hypersurfaces of both tautomers of adenine are very similar, although a basic difference emerges. While the photophysics related to the reaction paths involving the $^1(n\pi^*)$ and $^1(\pi\pi^*\ L_b)$ states will be similar in both systems and the minor changes observed will be dominated by small differences in geometries and relative energies for the computed minima, CIs, and reaction paths, in particular by the relatively low energy of the $^1(n\pi^*)$ state in 7*H*-adenine, a different behavior is predicted for the main decay pathway along the spectroscopic $^1(\pi\pi^*\ L_a)$ state. While in 9*H*-adenine most of the energy will rapidly decay to the ground state from the initially populated $H\rightarrow L$ $^1(\pi\pi^*\ L_a)$ state along a barrierless path and through a low-energy CI, $(gs/\pi\pi^*\ L_a)_{CI}$, in 7*H*-adenine the presence of a flat region in the PES and a local minimum with a twisted NH_2 moiety may prevent the ultrafast relaxation process. That region is also favorable for the transfer of population from the $^1(\pi\pi^*\ L_a)$ to the other two states, $^1(n\pi^*)$ and $^1(\pi\pi^*\ L_b)$, through the respective CIs. Compared to 9*H*-adenine, where no evidence for the NH_2-twisted minimum has been found, a large part of the population in the 7*H* tautomer will probably be distributed to the $^1(n\pi^*)$ and $^1(\pi\pi^*\ L_b)$ states, and this will disfavor direct ultrafast decay towards the ground state. As a result, an intrinsically distinct photophysical behavior can certainly be expected in the two compounds. The apparent absence of ultrafast decay and the larger fluorescence of 7-substituted adenines are in contrast to 9-substituted adenines, at least in aqueous media (see below). Apart from that, the present results emphasize the extreme impor-

tance of computing MEPs, the only accurate procedure, from the static viewpoint, to predict the photophysics of a molecule by properly connecting different regions of the PESs. To summarize, we conclude that the singlet photophysics of adenine and related compounds must be considered as a three-state problem involving two ππ*- and one nπ*-type singlet excited states.

Figures 6–10 display the geometries of the main stationary points of the hypersurfaces in both tautomers, while Tables 3 and 4 include the relative energies. The ground-

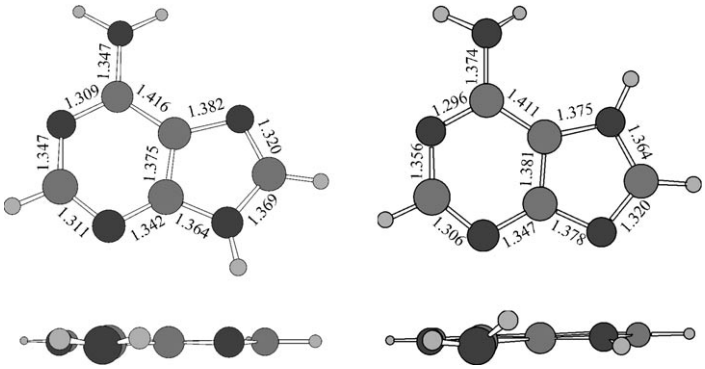

Figure 6. Structures and main bond lengths [Å] for the optimized ground states minima in 9*H*-adenine (left) and 7*H*-adenine (right).

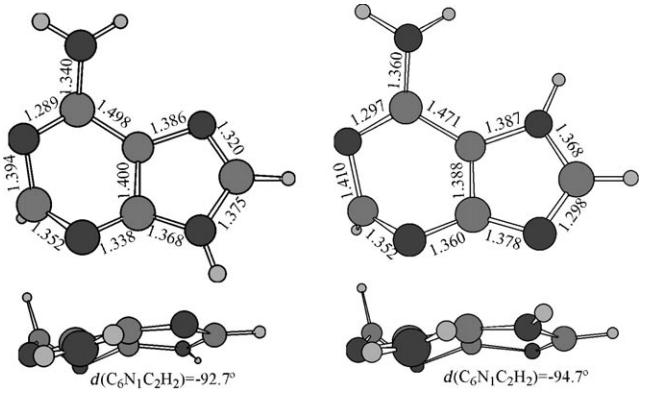

Figure 7. Structures, main bond lengths [Å], and dihedral angles [°] for the optimized (gs/ππ* L_a)$_{CI}$ in 9*H*-adenine (left) and 7*H*-adenine (right).

state minimum in both tautomers has an almost planar structure except for pyramidalization of the amino group. At the CASSCF level, 9*H*-adenine has dihedral angles $d(N^1C^6N^{10}H^{12}) = -9.6°$ and $d(N^1C^6N^{10}H^{11}) = -169.0°$, which increase in 7*H*-adenine to −10.7 and −144.1°, respectively. In particular, H^{11} goes out of plane, which causes an asymmetric pyramidalization that appears to be a common feature of all structures of the 7*H* tautomer because of the proximity of H^7 to the five-membered ring. This feature is the source of most of the differences found between 9- and 7-substituted adenines. Regarding the $^1(\pi\pi^*\ L_b)$ states minima, $^1(\pi\pi^*\ L_b)_{min}$, the only relevant change observed between the two tautomers is an increase in the pyramidalization of the amino group, with angles that change to −17.5 and −164.9°, respectively, for 9*H*-adenine, and to 9.4 and −113.3°, respectively, for 7*H*-adenine. The adiabatic energy T_e is slightly smaller (0.2 eV) for the latter. The surface is, however, very flat in that region, with out-of-plane frequencies for NH_2 of less than 400 cm^{-1}.[35] When the geometry is forced to be planar, the energy difference with respect to the $^1(\pi\pi^*\ L_b)_{min}$ structure is computed to be 1 kcal mol^{-1} (0.04 eV) higher. Finally, the minima of the $^1(n\pi^*)$ states, $^1(n\pi^*)_{min}$, show larger differences with respect to the previous structures. For 9*H*-adenine the six-membered ring deviates from planarity. The values of the most relevant dihedral angles are $d(N^3C^2N^1C^6) = -52.7$, $d(N^1C^6N^{10}H^{12}) = -15.4$, and $d(N^1C^6N^{10}H^{11}) = -157.0°$. On the contrary, for 7*H*-adenine the ring basically recovers planarity and, because of the presence of the hydrogen atom on N^7, the amino group aligns with the short axis of the molecule and adopts dihedral angles $d(N^1C^6N^{10}H^{12}) = -123.1°$ and $d(N^1C^6N^{10}H^{11}) = 106.5°$. This difference between the tautomers has major consequences for the adiabatic position of the $^1(n\pi^*)$ minima, computed at 4.52 eV in 9*H*-adenine and at 4.14 eV in 7*H*-adenine, and also in the description of the photophysics (see below). Figures 11 and 12 describe pictorially the basics of the low-energy photoinduced processes in 9*H*- and 7*H*-adenine, respectively.

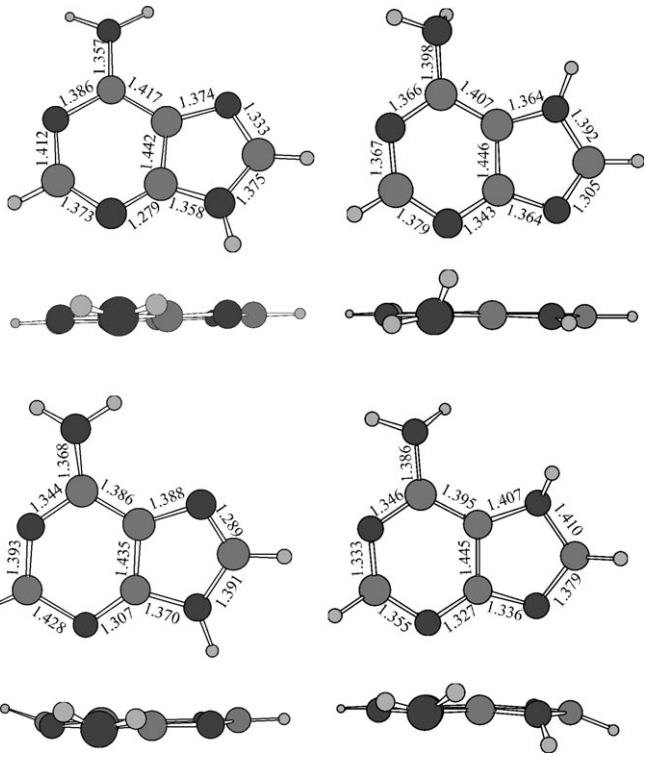

Figure 8. From top to bottom: structures and main bond lengths [Å] for the optimized ππ* L_b states minima and (ππ* L_b/nπ*)$_{CI}$ in 9*H*-adenine (left) and 7*H*-adenine (right).

As mentioned above, the reaction path (MEP) on the $^1(\pi\pi^*\ L_a)$ spectroscopic state leads to the conical intersection with the ground state, (gs/ππ* L_a)$_{CI}$. As shown in

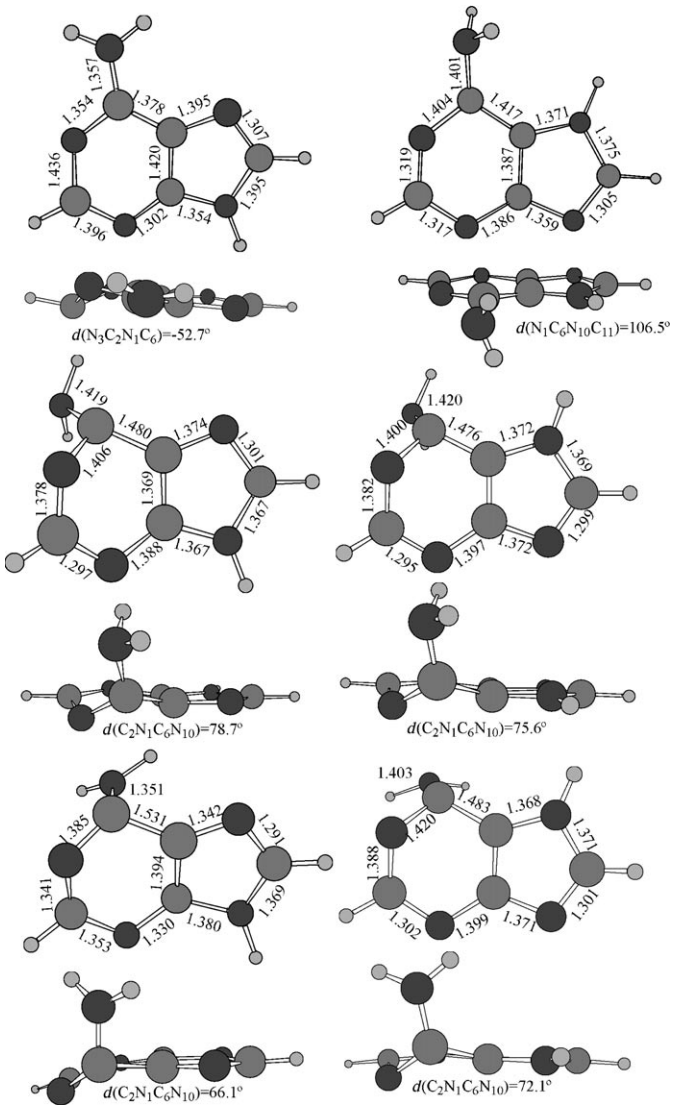

Figure 9. From top to bottom: structures and main bond lengths [Å] for the optimized $^1(n\pi^*)$ state minima $^1(n\pi^*)_{min}$, the $^1(n\pi^*)$ to $(gs/n\pi^*)_{CI}$ transition state $^1(n\pi^*)_{TS}$, and $(gs/n\pi^*)_{CI}$ in 9*H*-adenine (left) and 7*H*-adenine (right).

Figure 7, both tautomers exhibit similar out-of-plane deformations at the crossing, with dihedral angles of $d(C^6N^1C^2H^2) = -92.7°$ and $d(C^6N^1C^2H^2) = -94.7°$ for 9*H*- and 7*H*-adenine, respectively. The puckering of the $N^1C^2H^2N^3$ group in the six-membered ring is the common feature found in the lowest energy S_1/S_0 conical intersection connecting the lowest $\pi\pi^*$ and the ground state, $(gs/\pi\pi^*)_{CI}$, in other nucleobases such as cytosine[17,18] and uracil.[20] The presence of a $^1(\pi\pi^*\ L_a)$ barrierless path from the FC region towards $(gs/\pi\pi^*\ L_a)_{CI}$ provides an efficient mechanism for nonradiative relaxation to the ground state in which the CI structure behaves like a funnel for a decay with ultrashort lifetime. Considering that it involves the spectroscopic state, this is the primary deactivation pathway of excited adenine, in particular for the 9*H* tautomer. As explained above, 7*H*-adenine has a local minimum (cf. Figure 10) along the deactivation path from the FC excited $^1(\pi\pi^*\ L_a)$ state, and consequently the ultrafast decay will be perturbed and other pathways may become equally relevant. To check other possible internal conversion funnels, the accessibility of the low-lying and other CIs and the barriers found in the PES along the reaction paths must be computed (cf. Table 3 and 4).

Secondary pathways will depopulate the other two low-lying singlet excited states, $^1(n\pi^*)$ and $^1(\pi\pi^*\ L_b)$, activated through crossing along the $^1(\pi\pi^*\ L_a)$ MEP or by direct absorption. Regarding the crossings, we found for 9*H*-adenine the $(\pi\pi^*\ L_a/n\pi^*)_{CI}$ and $(\pi\pi^*\ L_a/\pi\pi^*\ L_b)_{CI}$ structures, which have intermediate geometries with slight pyramidalization of the six-membered ring and the amino group (see Supporting Information), and from which the system evolves towards the minima of their respective states. With respect to population by direct absorption, in the resonant multiphoton ionization (REMPI)[31–33] and laser-induced fluorescence (LIF)[31] jet-cooled spectra, the sharp lines detected at 4.40 and 4.48 eV were assigned to the band origins of the $^1(n\pi^*)$ and $^1(\pi\pi^*\ L_b)$ transitions, respectively, a state ordering confirmed for both tautomers by the present results (see Tables 1 and 2). Starting from the lowest minima in the S_1 hypersurface, $^1(n\pi^*)_{min}$, two different paths were explored. First, the $^1(n\pi^*)$ state connects through a transition state $^1(n\pi^*)_{TS}$ with the CI $(gs/n\pi^*)_{CI}$, and this makes repopulation

Table 3. Computed structures and energy differences for the low-lying singlet excited states of 9*H*-adenine at the CASPT2//CASSCF(12,11)/6-31G(d,p) level.[a]

Structure	Description	Energy differences [kcal mol^{-1}]			Energy differences [eV]		
		ΔE_1[b]	ΔE_2[c]	ΔE_3[d]	ΔE_1[b]	ΔE_2[c]	ΔE_3[d]
$(gs/\pi\pi^*\ L_a)_{CI}$	CI $^1gs/\pi\pi^*\ ^1L_a$	–	0.0[e]	1.6	–	0.00[e]	0.07
$(gs/n\pi^*)_{CI}$	CI $^1gs/^1n\pi^*$	1.6 [$^1(n\pi^*)$]	11.7	7.1	0.07 [$^1(n\pi^*)$]	0.51	0.31
$^1(n\pi^*)_{TS}$	TS $^1(n\pi^*)_{min}$–$(gs/^1n\pi^*)_{CI}$	1.9 [$^1(n\pi^*)$]	12.0	–	0.08 [$^1(n\pi^*)$]	0.52	–
$^1(n\pi^*)_{TS2}$	TS $^1(n\pi^*)_{min}$–$(gs/\pi\pi^*\ ^1L_a)_{CI}$	10.7 [$^1(n\pi^*)$]	20.1	–	0.46 [$^1(n\pi^*)$]	0.87	–
$(\pi\pi^*\ L_b/n\pi^*)_{CI}$	CI $\pi\pi^*\ ^1L_b/n\pi^*$	3.2 [$^1(\pi\pi^*\ L_b)$]	21.7	2.5	0.14 [$^1(\pi\pi^*\ L_b)$]	0.94	0.11
$(\pi\pi^*\ L_b/\pi\pi^*\ L_a)_{CI}$	CI $\pi\pi^*\ ^1L_b/\pi\pi^*\ ^1L_a$	5.3 [$^1(\pi\pi^*\ L_b)$]	23.8	3.0	0.23 [$^1(\pi\pi^*\ L_b)$]	1.03	0.13
$(n\pi^*/\pi\pi^*\ L_a)_{CI}$	CI $n\pi^*/\pi\pi^*\ ^1L_a$	19.8 [$^1(n\pi^*)$]	29.9	0.5	0.86 [$^1(n\pi^*)$]	1.30	0.02
$^1(n\pi^*)_{TS\ SP1}$[f]	TS $^1(n\pi^*)_{min}$–$(gs/\pi\pi^*\ ^1L_a)_{CI}$	−0.7 [$^1(n\pi^*)$]	9.4	–	−0.03 [$^1(n\pi^*)$]	0.41	–
$^1(n\pi^*)_{TS\ SP2}$[f]	TS $^1(n\pi^*)_{min}$–$(gs/^1n\pi^*)_{CI}$	3.0 [$^1(n\pi^*)$]	13.2	–	0.13 [$^1(n\pi^*)$]	0.57	–

[a] Transition states (TS): CASPT2//CASSCF level. Conical intersections (CI): CASPT2 scans. [b] Between the structure and the minimum of the mentioned state. [c] Between the structure and the reference $(gs/\pi\pi^*\ L_a)_{CI}$ energy. [d] At the CI (CASPT2 level). The average energy was used as reference. [e] At this level the conical intersection is located adiabatically with respect to the ground state at 4.09 eV. [f] CASSCF geometries from ref. [22].

Table 4. Computed structures and energy differences for the low-lying singlet excited states of 7*H*-adenine at the CASPT2//CASSCF(12,11)/6-31G(d,p) level.[a]

Structure	Description	Energy differences [kcal mol^{-1}]				Energy differences [eV]			
		ΔE_1[b]	ΔE_2[c]	ΔE_3[d]	ΔE_4[e]	ΔE_1[b]	ΔE_2[c]	ΔE_3[d]	ΔE_4[e]
$(gs/\pi\pi^* L_a)_{CI}$	CI $^1gs/\pi\pi^* {}^1L_a$	–	0.0[f]	0.6	7.1	–	0.00[f]	0.03	0.31
$(gs/n\pi^*)_{CI}$	CI $^1gs/n\pi^*$	−1.3 [$^1(n\pi^*)$]	2.6	6.4	–8.7	−0.06 [$^1(n\pi^*)$]	0.11	0.28	−0.38
$^1(n\pi^*)_{TS}$	TS $^1(n\pi^*)_{min}$–$(gs/n\pi^*)_{CI}$	2.4 [$^1(n\pi^*)$]	6.3	–	1.4	0.10 [$^1(n\pi^*)$]	0.27	–	0.06
$^1(n\pi^*)_{TS2}$	TS $^1(n\pi^*)_{min}$–$(gs/\pi\pi^* {}^1L_a)_{CI}$	10.6 [$^1(n\pi^*)$]	14.5	–	0.9	0.46 [$^1(n\pi^*)$]	0.63	–	0.04
$(\pi\pi^* L_b/n\pi^*)_{CI}$	CI $\pi\pi^* {}^1L_b/n\pi^*$	7.6 [$^1\pi\pi^* L_b$)]	22.4	0.6	6.7	0.33 [$^1(\pi\pi^* L_b)$]	0.97	0.03	0.29
$(\pi\pi^* NH_2)_{min}$	$^1(\pi\pi^*)_{min}$ twisted NH_2	118.3 [$^1(gs)$]	25.2	–	–	5.13 [$^1(gs)$]	1.09	–	–

[a] Transition states (TS): CASPT2//CASSCF level. Conical intersections (CI): CASPT2 scans. [b] Between the structure and the minimum of the mentioned state. [c] Between the structure and the reference $(gs/\pi\pi^* L_a)_{CI}$ energy. [d] At the CI (CASPT2 level). The averaged energy was used as reference. [e] From the equivalent structure of 9*H*-adenine. [f] At this level the conical intersection is located adiabatically with respect to the ground state at 4.00 eV.

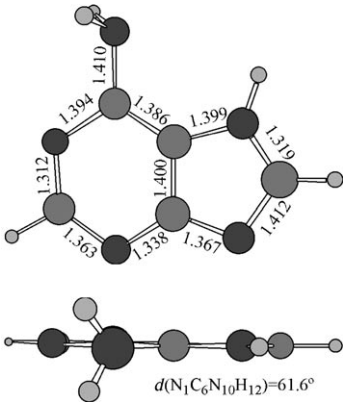

Figure 10. Structure and main bond lengths [Å] and dihedral angle [°] for the optimized $^1(\pi\pi^* L_a)$ state high-energy local minimum with twisted amino group $^1(\pi\pi^* L_a NH_2)_{min}$ in 7*H*-adenine.

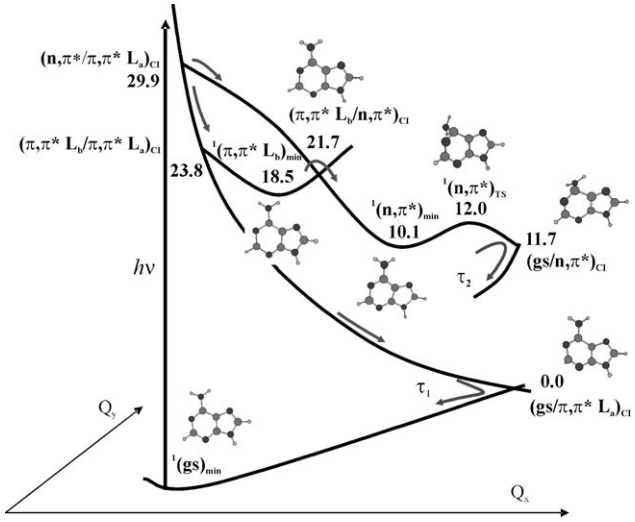

Figure 11. Scheme proposed on the basis of CASPT2 calculations for the main decay pathways of 9*H*-adenine, measured in molecular beams with intrinsic lifetimes $\tau_1 < 100$ fs and $\tau_2 \approx 1$ ps.[10] Energies in kcal mol^{-1} referred to the lowest conical intersection (for values in eV, see Table 3).

of the ground state possible. In 9*H*- and 7*H*-adenine, the barriers to accessing $^1(n\pi^*)_{TS}$ from $^1(n\pi^*)_{min}$ are computed to be 1.9 and 2.4 kcal mol^{-1} (0.08 and 0.10 eV), respectively,

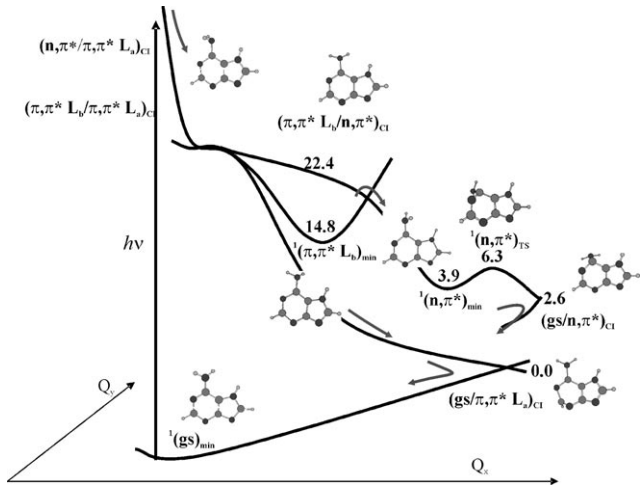

Figure 12. Scheme proposed on the basis of CASPT2 calculations for the main decay pathways of 7*H*-adenine. Energies in kcal mol^{-1} referred to the lowest conical intersection (for values in eV, see Table 4).

while the CIs are found slightly above (1.6 kcal mol^{-1}, 0.07 eV) and below (−1.3 kcal mol^{-1}, 0.06 eV) the respective minimum. The evolution of the reaction path $^1(n\pi^*)_{min}$–$^1(n\pi^*)_{TS}$–$(gs/n\pi^*)_{CI}$ (see Figure 9) mainly involves torsion of the C^6N^1 bond, which makes the amino group almost perpendicular to the purine ring. In 9*H*-adenine the dihedral angle $d(C^2N^1C^6N^{10})$ changes in the previous sequence −152.8, 78.7, and 66.1°, respectively, while in 7*H*-adenine the values are −162.5, 75.6, and 72.1°, respectively. For the 7*H* tautomer, while the amino group hydrogen atoms remain parallel to the short axis of the rings in the minimum and transition-state structures, they recover a long-axis position in the conical intersection.

Other evolution paths were explored from $^1(n\pi^*)_{min}$ (cf. Tables 3 and 4). New transition-state structures $^1(n\pi^*)_{TS2}$ that adiabatically connect the lowest minimum and the $(\pi\pi^* L_a)$ path were computed at 10.7 and 10.6 kcal mol^{-1} (0.46 and 0.45 eV) above $^1(n\pi^*)_{min}$ in 9*H*- and 7*H*-adenine, respectively. In 9*H*-adenine the computed $^1(n\pi^*)_{TS2}$ geometry shows nonplanarity of the six-membered ring, with dihedral angles of $d(C^6N^1C^2H^2) = -136.7°$ and $d(N^3C^2N^1C^6) = 69.4°$. On the contrary, for 7*H*-adenine, the structure of the rings is

almost planar, while the amino group hydrogen atoms are oriented along the short axis. Two other transition-state structures were taken from recent CASSCF optimizations in 9*H*-adenine, named SP1 and SP2[22] (hereafter $^1(n\pi^*)_{TSSP1}$ and $^1(n\pi^*)_{TSSP2}$), and used in our CASPT2 calculations, in order to make a straightforward comparison. The $^1(n\pi^*)_{TSSP1}$ conformation is similar to $^1(n\pi^*)_{TS2}$, although a different bond alternation is observed in the rings and the C^6N^{10} bond is 0.04 Å shorter. All required geometries can be found in the Supporting Information. As previously,[22] the $^1(n\pi^*)_{TSSP1}$ structure is not a transition state at the highest CASPT2 level, and lies lower in energy than $^1(n\pi^*)_{min}$ by 0.7 kcal mol^{-1} (0.03 eV). Other energy differences are included in Tables 3 and 4. Considering the accuracy of the approach, our results therefore describe two connections through which deactivation of the energy from the lowest gas-phase minimum at the S_1 hypersurface $^1(n\pi^*)_{min}$ will be favorable: the transition state $^1(n\pi^*)_{TS}$ towards the conical intersection with the ground state $(gs/n\pi^*)_{CI}$, and the transition state $^1(n\pi^*)_{TSSP1}$ connecting adiabatically the S_1 $^1(n\pi^*)_{min}$ and $^1(\pi\pi^*\ L_a)$ hypersurfaces and leading to the lowest conical intersection $(gs/\pi\pi^*\ L_a)_{CI}$.

The hypersurface around $^1(\pi\pi^*\ L_b)_{min}$ was also explored. No direct connection with the ground state (i.e., an S_1/S_0 conical intersection) was found. The search leads instead to breaking of the six-membered ring. A low-energy S_2/S_1 conical intersection was, however, located connecting the $^1(\pi\pi^*\ L_b)$ and $^1(n\pi^*)$ states, $(\pi\pi^*\ L_b/n\pi^*)_{CI}$. The CI is found 3.2 and 7.6 kcal mol^{-1} (0.14 and 0.33 eV) above $^1(\pi\pi^*\ L_b)_{min}$ in 9*H*- and 7*H*-adenine, respectively. Their structures are clearly somewhat in between the minima of both states, that is, the molecule is not far from planarity, like the $^1(\pi\pi^*\ L_b)$ states minima, but shows slight pyramidalization of the six-membered ring, similar to the optimized $^1(n\pi^*)$ states. The largest deviations from planarity come from the dihedral angles $d(C^6N^1C^2H^2) = -157.0°$ in 9*H*-adenine and $d(C^4C^5N^7H^7) = -131.7°$ in 7*H*-adenine (see Figure 8). This CI has been recently described for the 9*H* tautomer[22] and claimed many times in the past[47] as the key structure to explain the ultrafast deactivation of adenine. This interpretation is probably erroneous, because the predominant role of the $^1(\pi\pi^*\ L_a)$ state has been ignored. It is true that the computed small barriers and the structures similar to those of the $^1(\pi\pi^*\ L_b)$ states make $(\pi\pi^*\ L_b/n\pi^*)_{CI}$ easily accessible after optical population and allow partial deactivation of the $^1(\pi\pi^*\ L_b)$ states. However, most of the energy has already relaxed to the ground state through $(gs/\pi\pi^*\ L_a)_{CI}$, the main deactivation path.

Other structures and reaction paths were also explored, for instance, the suggested NH dissociation along a repulsive $^1(\pi\sigma^*)$ state correlating with the ground state of the hydrogen-abstracted radical.[13,48,49,50] The energy of the dissociation channel, computed here adiabatically 4.40 eV above the ground state in the 9*H* tautomer, is also a lower limit for the conical intersection of $^1(\pi\sigma^*)$ with the adenine ground state. The corresponding decay mechanism cannot be competitive with the previously described ultrafast barrierless $^1(\pi\pi^*\ L_a)$ path through $(gs/\pi\pi^*\ L_a)_{CI}$, which lies at 4.09 eV. This mechanism will be discussed later. On the other hand, the role of amino-group twisting was suggested earlier.[47] In 9*H*-adenine we only found evidence of low-energy twisting of the NH_2 group along the $^1(n\pi^*)_{min}$–$^1(n\pi^*)_{TS}$–$(gs/n\pi^*)_{CI}$ pathway. In 7*H*-adenine, however, the twisting coordinate enters easily into the photophysical scheme because of the interaction with H^7, and different twisted conformations can be reached. In particular, the local $^1(\pi\pi^*\ L_a\ NH_2)_{min}$ minimum, with the NH_2 group twisted almost 60° and adiabatically 5.13 eV from the ground-state minimum, is found along the $^1(\pi\pi^*\ L_a)$ path. The suggested contribution in free adenine of a twisted intramolecular charge transfer (TICT) mechanism as source of ultrafast internal conversion[51,52] can be disregarded. Indeed, no evidence has been so far found in adenine derivatives such as *N*,*N*-dimethyladenine.[10] On the contrary, twisting of the NH_2 group seems to interfere with ultrafast decay in 7-substituted adenines. A full comment on the photophysics of the system is addressed in the next section.

Photophysics of adenine: The photophysics of adenine is very rich, whether under isolated conditions, in solvated environments, or integrated in polynucleotide chains. We start our discussion with the data measured in molecular beams. Figures 11 and 12 help in rationalizing the experimental observations by summarizing the present three-state model proposed for adenine. After controversial debate,[1] and also by comparison with the methyl derivatives, several of the sharp vibronic transitions observed in the IR/UV,[34] REMPI,[31–33] LIF,[31] and dispersed fluorescence (DF)[53] spectra of jet-cooled adenine, in particular the features observed at 35 503 cm^{-1} (4.40 eV) and at 36 105 cm^{-1} (4.48 eV), were assigned to the origin of $^1(n\pi^*)$- and $^1(\pi\pi^*)$-type transitions in the 9*H* tautomer, respectively. This conclusion is supported by the present calculations, which identify the latter as the $^1(\pi\pi^*\ L_b)$ state of 9*H*-adenine, and place the origin of the lowest $^1(n\pi^*)$ transition below the $^1(\pi\pi^*\ L_b)$ band origin. The two minima differ noticeably in geometry, but they belong to the S_1 hypersurface. The vibronic peaks are observed in a narrow energy range and with origins more closely spaced than expected. This observation can be explained by the presence of our computed conical intersection $^1(\pi\pi^*\ L_b/n\pi^*)_{CI}$ lying (see Table 3) just a few kcal mol^{-1} above $^1(\pi\pi^*\ L_b)_{min}$. The peaks related to the $^1(\pi\pi^*\ L_b)$ state are anyway much more intense than those involving the $^1(n\pi^*)$ state. In the nearby region, vibronic coupling between the states will increase, involving out-of-plane modes for the $N^1C^2N^3$ group and enhancing the intensity of the otherwise weak $^1(n\pi^*)$ peaks. The $^1(\pi\pi^*\ L_b)$ state is, however, expected to be much more populated than the $^1(n\pi^*)$ state.

The striking fact that none of the vibronic lines of the REMPI spectrum could be assigned to a second $^1(\pi\pi^*)$-type excited state, which, as observed in Table 1, lies slightly above the $^1(\pi\pi^*\ L_b)$ state in the FC region, has been repeatedly stressed.[1] The results reported here clearly show (Fig-

ures 2 and 11) that for 9*H*-adenine the $^1(\pi\pi^*\ L_a)$ state has a repulsive character, with no minimum in the PES, a fact that explains the absence of corresponding vibronic resonances. On the other hand, the presence in the spectrum of weak peaks between the two assigned origins, in particular at 35824 cm^{-1} (4.44 eV), associated with the minor 7*H* tautomer has been also proposed.[33] Certainly, our calculations place the origin of the 7*H*-adenine $^1(\pi\pi^*\ L_b)$ state 0.2 eV below that of the 9*H* tautomer. Although the contribution of the 7*H* form to the overall spectrum is expected to be small (especially after jet cooling[32]), the presence of related bands can be explained because the corresponding intensity for the $^1(\pi\pi^*\ L_b)$ transition is five times larger in 7*H*- than in 9*H*-adenine (see Tables 1 and 2). It is unlikely that those bands belong to the 7*H*-adenine $^1(n\pi^*)$ transition, because the equivalent peaks of the 9*H* tautomer are weaker and, in particular, because our CASPT2 results place the 7*H*-adenine $^1(n\pi^*)$ origin nearly 3000 cm^{-1} (0.4 eV) below the 9*H*-adenine band origin. A full characterization of the peaks must wait until high-resolution experiments are available in which the rotational structure of the bands is analyzed and the direction of the electronic transition dipole moment compared with the results of ab initio calculations.

The most interesting features in the photophysics of the DNA/RNA nucleobases are the ultrashort radiationless decay times obtained both for jet-cooled and solvated species. Early experiments on base monomers in aqueous solution (see a recent careful review[1]) proved that S_1 lifetimes were short, well below the experimental time resolution at that time, typically 1 ps. The measured short decay times are consistent with the broad and diffuse bands observed about 1100 cm^{-1} (3.1 kcal mol^{-1}, 0.13 eV) above the $^1(\pi\pi^*\ L_b)$ origin in the molecular beam experiments, precisely the energy needed to reach the conical intersection $^1(\pi\pi^*\ L_b/n\pi^*)_{CI}$ from $^1(\pi\pi^*\ L_b)_{min}$ in 9*H*-adenine (3.2 kcal mol^{-1}, 0.14 eV). Excited-state dynamics studies on isolated nucleobases were recently performed by measuring fluorescence lifetimes or by time-resolved pump-probe REMPI detection with different time resolutions. Kang et al.[15,54] reported the first pump–probe mass spectroscopy study with femtosecond pulses on the nucleobases at an excitation energy of 267 nm (4.64 eV), describing a single exponential decay with state lifetimes close to 1 ps for adenine, 9-methyladenine, 7-methyladenine, and their deuterated counterparts. More recently, two detailed characterizations of the excited-states relaxation dynamics of adenine in the gas phase have been reported. Ullrich et al.[55,56] used time-resolved photoelectron spectroscopy (TRPES) in several DNA and RNA bases to determine electronic decay channels after excitation at certain wavelengths corresponding to different population conditions in the initially excited states, in particular at 250 nm (4.95 eV), 267 nm (4.64 eV), and 277 nm (4.48 eV). Canuel et al.,[10] on the other hand, employed mass-selected femtosecond pump–probe transient resonant ionization (TRI) spectroscopy to investigate the decay mechanisms of the nucleobases and several methyl derivatives after excitation at 267 nm (4.64 eV). Probably because of the different time resolutions employed (160 and 80 fs, respectively), the conclusions obtained from the two experiments slightly differ.

In the TRPES study on gas-phase adenine,[55,56] excitations at 250 and 267 nm led to at least two deactivation channels with ultrashort (<50 fs) and intermediate (750 fs) lifetimes. In their analysis, the authors assumed the initial excitation of a bright $^1(\pi\pi^*)$ state, rapidly (<50 fs) depopulated by internal conversion towards the lower lying $^1(n\pi^*)$ state, which, in turn, decays to the ground state in 750 fs. Excitation at 267 nm, on the other hand, resulted in an additional decay with a lifetime shorter (<50 fs) than the experimental resolution, suggested to correlate with a NH-dissociative $^1(\pi\sigma^*)$ state. At 277 nm, supposedly close to the $^1(\pi\pi^*\ L_b)$ band origin, a single and large excited-state lifetime of >2 ps was extracted and related to the lowest triplet $^3(\pi\pi^*)$ state. The two channels obtained at 250 and 267 nm (50 and 750 fs) and the single channel found at 277 nm (>2 ps) were reported with similar lifetimes for the other nucleobases. Instead of the single (Kang et al.[15,54]) or triple (Ullrich et al.[55,56]) exponential fittings used earlier, Canuel et al.[9] selected, in their TRI study at 267 nm, a double exponential fitting leading to ultrafast (100 fs) and intermediate (1.1 ps) components. The measurements were extended to 9-methyladenine and *N*,*N*-dimethyladenine, and the corresponding decay times were 110 fs and 1.3 ps for the former, and 200 fs and 3.1 ps for the latter. These two lifetimes can be directly related to those previously reported for adenine near 50 fs and 750 fs,[55,56] while, in less resolved studies,[15,54] only a long-lived channel close to 1 ps seems to be detected. All these data have been interpreted by Canuel et al.[9] in terms of the same two-state model: once the spectroscopic state is populated, the 100 fs step would correspond to internal relaxation of the $^1(\pi\pi^*)$ state towards its minimum, followed by a slower step of 1.1 ps assigned for a switch to the $^1(n\pi^*)$ state and further relaxation to the ground state through a $(gs/n\pi^*)_{CI}$ conical intersection.

Focusing on our computed results, we propose the following photophysical scheme (Figures 11 and 12) based on a three-state model. Isolated, jet-cooled adenine seems to be basically composed of the 9*H* tautomer.[32,34] The key feature of its photophysics is the repulsive nature of the bright $^1(\pi\pi^*\ L_a)$ state which relaxes from the FC region to a low-lying funnel involving the ground state, $(gs/\pi\pi^*\ L_a)_{CI}$, in a barrierless manner. Along the minimal-energy path, another two PES corresponding to the $^1(n\pi^*)$ and $^1(\pi\pi^*\ L_b)$ states are crossed. Considering that $^1(\pi\pi^*\ L_a)$ is implied in the most strongly allowed transition dominating the low-lying absorption spectrum, most of the energy acquired by illuminating the molecule will rapidly decay along its hypersurface to the ground state, quenching the fluorescence. At excitation energies such as 250 or 267 nm, the $^1(\pi\pi^*\ L_a)$ state, which lies higher than the other two in the FC region, will be directly and largely populated. The presence of an ultrashort lifetime between 50 and 100 fs can therefore be explained by fast internal conversion to the ground state. We think that the ultrafast decay which is always recorded at energies higher than 267 nm should be better attributed to the $^1(\pi\pi^*\ L_a)$

state, which carries most of the population, instead of to the $^1(\pi\pi^*\ L_b)$ state. The additional 50 fs channel reported by Ullrich et al.[55,56] after excitation at 267 nm can, however, be assigned to energy relaxation from the less populated $^1(\pi\pi^*\ L_b)$ state towards its minimum. This alternative seems more plausible than the suggested assignment to the $^1(\pi\sigma^*)$ dissociative state, which correlates in the FC region with a higher lying and weak Rydberg transition[21] and at long distances with the hydrogen-abstracted radical, which, as explained, places the corresponding conical intersection $(gs/\pi\sigma^*)_{CI}$ at least 7.2 kcal mol^{-1} (0.31 eV, lower bound) above the lowest channel described here. The energy barriers to access the $^1(\pi\sigma^*)$ state from the FC region and along the dissociation distance have been estimated at about 5.4–5.5 eV.[21] The energies used in recent experiments which support the H^9-atom loss dynamics, from 280 to 239.5 nm (4.43–5.18 eV),[57,58] are clearly unable to surmount the barriers to the $^1(\pi\sigma^*)$ state in gas-phase adenine, except by direct absorption, adiabatically, at geometries with large NH bond lengths. The required energies, the presence of very similar decay mechanisms and times to those of adenine in derivatives like 9-methyladenine or *N*,*N*-dimethyladenine,[10] and the absence of kinetic isotope effects[1,54,59] indicate that the different NH dissociation channels cannot be responsible for the ultrafast decays in isolated nucleobases at low energies, which should be better related to the $^1(\pi\pi^*)$ channels. The presence of photolyzed hydrogen atoms after excitation of adenine and 9-methyladenine at low energies, however, opens new doors to be explored. Hünig et al.[58] using three-photon REMPI spectroscopy at 243.1 nm (5.10 eV) deduced an NH dissociation energy of 4.46 eV for 9*H*-adenine. On the other hand, Zierhut et al.[57] used excitation energies as low as 266 nm (4.66 eV) and estimated a dissociation energy of 4.07 eV. As in the previous DFT/MRCI study,[21] the present results, which place the dissociation limit at 4.40 eV, better support the experimentally derived energy of 4.46 eV, obtained by exciting the molecule at 5.10 eV. New calculations and experiments are required, especially to check the possibility of tunneling and isotope effects in the H-loss processes. At present, it can be concluded that the $^1(\pi\sigma^*)$ path is probably not related to the already measured ultrafast relaxation processes in adenine and its nucleosides and nucleotides, although it can be certainly related to other fast decay processes at higher energies[50] and in base pairs.[60]

It would be particularly informative to carry out experiments on 7-methyladenine in molecular beams at the level recorded by Canuel et al.[10] in their TRI measurements. They reported an ultrafast decay (110 fs) in 9-methyladenine, which has been also found in solution. However, as will be discussed below, it is unclear whether the 7-substituted species also undergo fast decay or, as predicted by our calculations on 7*H*-adenine, relaxation along the $^1(\pi\pi^*\ L_a)$ state may be inactivated by the presence of a local minimum in the region where the path crosses with the $^1(n\pi^*)$ and $^1(\pi\pi^*\ L_b)$ states. Such measurements are strongly encouraged.

In any case, it is clear that in 9*H*-adenine, predominant under molecular-beam conditions, the 50–100 fs decays are related to relaxation within the $^1(\pi\pi^*)$ states. When the excitation energy is decreased to 277 nm, near the origin of the $^1(\pi\pi^*\ L_b)$ state, the ultrafast deactivation disappears. The second, longer lived decay (750 fs to 1.1 ps) observed in the 250 and 267 nm experiments can be better attributed to the decay process related to both the $^1(\pi\pi^*\ L_b)$ and $^1(n\pi^*)$ states. At high excitation energies, the $^1(\pi\pi^*\ L_b)$ and $^1(n\pi^*)$ states will be basically populated through crossing with the $^1(\pi\pi^*\ L_a)$ PES and, to a minor extent, by direct absorption, in particular the transition to $^1(\pi\pi^*\ L_b)$, which carries more intensity. The decay proceeds from $^1(\pi\pi^*\ L_b)_{min}$ via a state switch to the $^1(n\pi^*)$ state and reaches its minimum (the lowest on the S_1 PES), from which several relaxation pathways are possible: first, following the N^1C^6 bond torsion coordinate (NH_2 perpendicular to the ring) and via the $^1(n\pi^*)_{TS}$ transition state through the conical intersection $(\pi\pi^*\ L_b/n\pi^*)_{CI}$, and, second, involving torsion of C^2N^3 (pyramidalization of the ring) through the transition state $^1(n\pi^*)_{TSSP1}$ connecting $^1(n\pi^*)_{min}$ with the $^1(\pi\pi^*\ L_a)$ hypersurface. The preferred pathway will be reached after a subtle balance between the available excess vibrational energy and the barrier heights. Considering the reported[10] large increase of the longer lifetime from adenine (1.1 ps) to *N*,*N*-dimethyladenine (3.1 ps), while 9-methyladenine remains similar (1.3 ps), the most plausible hypothesis points to the main role of the $^1(n\pi^*)_{TS}$ structure and the $(gs/n\pi^*)_{CI}$ funnel, where the amino group has to reach a perpendicular conformation, and that model was used to construct Figures 11 and 12. The same conclusion is indicated by the measurements at 277 nm, at the origin of $^1(\pi\pi^*\ L_b)$, in which the ultrafast decays disappear and large decay lifetimes are reported with 9 ps[32] and >2 ps.[55,56] The lack of excess vibrational energy by direct population of the $^1(\pi\pi^*\ L_b)_{min}$ structure leads to a slow decay, after switching to the $^1(n\pi^*)$ state first, and towards the $(gs/n\pi^*)_{CI}$ conical intersection later. The decrease of the ion signal observed in the REMPI spectrum[32] at longer times can be explained by the decrease of the intensity associated with switching of the $^1(\pi\pi^*\ L_b)$ to the $^1(n\pi^*)$ state. The present model does not require introduction of an intersystem crossing mechanism to explain the observed decay processes.[55,56] Regarding the differences between the two computed adenine tautomers, the stabilization of the $^1(\pi\pi^*\ L_b)$ state in 7*H*-adenine and the increase of the $^1(\pi\pi^*\ L_b)_{min}$–$(\pi\pi^*\ L_b/n\pi^*)_{CI}$ barrier from 3.2 (9*H*-adenine) to 7.6 kcal mol^{-1} (7*H*-adenine) (0.14 and 0.33 eV), leads to the prediction of longer lifetimes for the second decay in 7*H*-adenine, as measured by Kang et al.[54] from 9- to 7-methyladenine.

The behavior of adenine and its derivatives in solution or integrated in polynucleotide chains is somewhat, although not much, different from that under isolated conditions. Adenine has been measured to produce weak fluorescence in aqueous environments with band origin near 280 nm (4.43 eV), band maxima from 306 to 321 nm (4.05 to 3.86 eV), and quantum yields ϕ_F of 2.6×10^{-4} to 3.3×10^{-4}.[2–7]

Compared with our computed isolated-molecule values, the observed fluorescence in solution can be attributed to the $^1(\pi\pi^*\ L_b)$ state, which is not the initially populated state. The computed radiative lifetimes for 9*H*- and 7*H*-adenine, derived by means of the Strickler–Berg relationship, of 251 and 54 ns, respectively, can be compared with experimentally estimated data, between 3.9 and 34 ns.[6,7,59] The results suggest, as was classically supposed,[7] that the $^1(\pi\pi^*\ L_b)$ state of the 7*H* tautomer, the population of which increases in polar solvents because of its larger dipole moment, is the real source of fluorescence. Regarding the measured lifetimes in solution, adenine has biexponential decays in the femtosecond transient absorption spectra with intrinsic fluorescence lifetimes of 180 fs and 8.8 ps.[59] The data agree with the fluorescence up-conversion results, 230 fs and 8.0 ps.[61] Under jet-cooled conditions 9- and 7-methyladenine were reported first with a similar single decay near 1 ps,[15,54] while 9-methyladenine was later more accurately measured with two decays, at 110 fs and 1.3 ps.[10] It seems that the slow component disappears for solvated 9-substituted compounds, while the ultrafast relaxation is lost in 7-substituted adenines. In the light of our results, the disappearance of the fast component in 7*H*-adenine can be related to the presence of the $^1(\pi\pi^*\ L_a\ NH_2)_{min}$ region, where the fast decay may be deactivated and part of the population transferred to the $^1(\pi\pi^*\ L_b)$ and $^1(n\pi^*)$ states. In the meanwhile, the fast decay measured in aqueous adenine is attributed to the nonemitting deactivation process along the $^1(\pi\pi^*\ L_a)$–$(gs/\pi\pi^*\ L_a)_{CI}$ pathway, and corresponds basically to the major (9*H*) and not the minor (7*H*) tautomer.

Summary and Conclusions

Ab initio multiconfigurational second-order perturbation theory (CASPT2 approach) was employed to compute potential energy hypersurfaces for the low-lying singlet excited states of the most stable tautomers of adenine: 9*H*-adenine and 7*H*-adenine. Equilibrium geometries (min), minimum-energy reaction paths (MEP), transition states (TS), and conical intersections (CI) were computed in order to elucidate the photophysics of the molecule. The present calculations, together with other recent theoretical studies on 9*H*-adenine,[21,22] bring to light a three-state model able to rationalize the experimental findings, involving two $^1(\pi\pi^*)$, $^1(\pi\pi^*\ L_a)$, and $^1(\pi\pi^*\ L_a)$ states and one $^1(n\pi^*)$ state, the last-named related to the nitrogen atoms of the six-membered ring, and two S_0/S_1 conical intersections, labeled $(gs/\pi\pi^*\ L_a)_{CI}$ and $(gs/n\pi^*)_{CI}$. Figures 11 and 12 help to understand the scheme proposed here. Adenine photophysics in molecular beams can be understood by simply including the predominant tautomer under these conditions, 9*H*-adenine, within the model. At excitation energies of at least 267 nm (4.64 eV) or higher, the initially populated state is identified as the spectroscopic $^1(\pi\pi^*\ L_a)$ singlet state, which carries most of the population. Along the minimum-energy path, a barrierless funnel with the ground state is found at low energies corresponding to the conical intersection $(gs/\pi\pi^*\ L_a)_{CI}$ responsible for the ultrafast decay measured in jet-cooled and solvated adenine near 100–200 fs, also found in adenosine, and adenosine monophosphate. This relaxation mechanism, triggered by out-of-plane vibrational modes corresponding to puckering of the six-membered ring (rotation of the C^2N^3 bond), and not the earlier claimed vibronic coupling between $^1(\pi\pi^*\ L_b)$ and $^1(n\pi^*)$ states, is the key feature responsible for most of the emission quenching observed in adenine, as well as in other nucleobases. The presence of the spectroscopic $^1(\pi\pi^*\ L_a)$ transition (with the largest oscillator strengths at low energies) was traditionally ignored. The additional ultrafast channel found only after 267 nm excitation should be better related to the intrinsic relaxation of the $^1(\pi\pi^*\ L_b)$ state. A secondary decay channel, reported to have longer lifetimes, is observed also in jet-cooled adenine at 1.1 ps. The mechanism proposed for energy relaxation involves population of the $^1(\pi\pi^*\ L_b)$ and $^1(n\pi^*)$ states, either by crossing with the $^1(\pi\pi^*\ L_a)$ path through the conical intersections $(\pi\pi^*\ L_a/\pi\pi^*\ L_b)_{CI}$ and $(\pi\pi^*\ L_a/n\pi^*)_{CI}$ or by direct excitation, as proved by the assignments, confirmed here, of the absorption peaks of the REMPI and LIF spectra in jets. Once populated, essentially the $^1(\pi\pi^*\ L_b)$ state, there is a state switch to the $^1(n\pi^*)$ state through the conical intersection $(\pi\pi^*\ L_b/n\pi^*)_{CI}$ reaching $^1(n\pi^*)_{min}$, and from there the system evolves through the $^1(n\pi^*)_{TS}$ transition state to the $(gs/n\pi^*)_{CI}$ funnel, ultimately responsible for internal conversion to the ground state. The role of this mechanism in the second, longer-lived decay can be confirmed by considering that, at both the saddle point and the crossing, the amino group becomes almost perpendicular to the rings, a structure that explains the increase of the lifetime up to 3.1 ps in *N*,*N*-dimethyladenine, with two methyl groups moved out of plane, while it remains similar in 9-methyladenine (1.3 ps). The same relaxation mechanism is responsible for the unique increased lifetime (>2 ps) measured at an excitation energy of 277 nm (4.48 eV), band origin for the $(\pi\pi^*\ L_b)$ transition. The reduced excess of vibrational energy leads to a much slower decay process.

Measurements on adenine and several derivatives in condensed phases can be only rationalized when the more polar and stabilized 7*H* tautomer is taken into account. As shown by the present calculations, there are three basic differences between the two tautomers. First, the reaction path for deactivation of the initially populated $^1(\pi\pi^*\ L_a)$ state in 7*H*-adenine reaches a flat plateau where the barrierless ultrafast decay typical of 9-subtituted adenines slows down, and transfer of energy to the $^1(\pi\pi^*\ L_b)$ and $^1(n\pi^*)$ states becomes favorable. This feature adequately explains the absence of ultrafast decay reported up to now for 7-substituted adenines, both isolated and in aqueous media, and stresses the key importance of computing MEPs that accurately connect the different PES regions. Second, the $^1(\pi\pi^*\ L_b)$ and $^1(n\pi^*)$ states minima are located lower in 7*H*-adenine by 0.23 and 0.38 eV, respectively, and, third, the barrier to switching between the two states, that is, the energy difference between $^1(\pi\pi^*\ L_b)_{min}$ and $(\pi\pi^*\ L_b/n\pi^*)_{CI}$, is

4.4 kcal mol^{-1} (0.19 eV) higher in 7*H*-adenine. The suggested predominance of 7*H*-adenine in the fluorescence of aqueous adenine is understood by considering the larger energy needed to escape from $^1(\pi\pi^*\ L_b)_{min}$, also confirmed as the fluorescent state by comparison of the computed (54 ns) and experimental (34 ns) radiative lifetimes, which are one order of magnitude larger for the other states. Although to accurately study the decay mechanisms in solvation more sophisticated theoretical models are required, qualitatively the presence of two deactivation channels in room-temperature aqueous adenine can be attributed to the $^1(\pi\pi^*\ L_a)$ (subpicosecond decay) and the $^1(\pi\pi^*\ L_b)$–$^1(n\pi^*)$ (picosecond decay) paths, the former due to the 9*H*-tautomer, and the latter only accessible to the 7-substituted species because of the lower energy of the $^1(n\pi^*)$ state in this case. In low-temperature experiments, where the vibrational energy has decreased, the latter mechanism leads to decays increased up to nanoseconds. The presence of other deactivation channels related to the suggested repulsive $^1(\pi\sigma^*)$ path is not confirmed at low energies for the isolated systems. On the contrary, the predominant role of a $\pi\pi^*$-type state on the ultrafast deactivation of adenine is strongly supported.

As a consequence of the present analysis, and apart from specific conclusions about photoinduced mechanisms in adenine, we can confirm that determining the detailed photophysics of DNA/RNA nucleobases is a complex task requiring both accurate experimental and theoretical parameters, which must be interpreted together. Unfortunately, the ultimate photophysical mechanisms depend on subtle differences in the topology of the PES and the experimental conditions. Simple models based on energy gaps, either vertical or adiabatic, such as the so-called "proximity effect"[62,63,64] are not helpful in most cases. For instance, considering the decrease in the energy gaps in solution, the proximity effect, that is, weak vibronic coupling in regions of avoided crossing between $^1(\pi\pi^*\ L_b)$ and $^1(n\pi^*)$ states inducing coupling with higher lying vibrational levels of the ground state, predicts slower nonradiative decays in water, which is at odds with the experimental observations.[1] In particular for adenine, the coupling of the $^1(\pi\pi^*\ L_b)$ and $^1(n\pi^*)$ states, used as model by many authors,[47,65,66] is not the main reason for quenching of the fluorescence, but the presence of low-lying and easily accessible conical intersections $(gs/\pi\pi^*\ L_a)_{CI}$, which deactivate the strongly populated state. Many calculations have been performed to support the proximity-effect hypothesis in which the out-of-plane vibrations are mentioned as acting as coupling coordinates to quench emission. None of those studies, all of which lack quantitivity because of the use of methods without inclusion of dynamic correlation, explained how the ground state was finally reached, and, most importantly, the main deactivation path along the strongly allowed $^1(\pi\pi^*\ L_a)$ state was missing. Only recently, CASPT2//CASSCF[22] and DFT/MRCI[21] calculations on 9*H*-adenine included conical intersections and the presence of a low-lying $(gs/\pi\pi^*\ L_a)_{CI}$ deactivation funnel within the model. Together with the present calculations, in which other deactivation paths are proposed in both 9*H*- and 7*H*-adenine, the theoretical description now constitutes a solid foundation for interpreting the observed data, within the perspective of a static view. Based on the present and similar quantum chemical studies, work in the future should be focused in two directions: a more accurate theoretical determination of the molecular properties in solution, still an unsolved task today, and extensive calculations including the dynamical aspects of the problem.

Acknowledgements

The research reported has been financed by project FEDER-MEC CTQ2004-01739 and by the Generalitat Valenciana (GV06/192). A.C.B. thanks CNPq (Brasilian Research Council) for a research fellowship, FAPESP (Fundaçaõ de Amparo à Pesquisa do Estado de São Paulo) for financial support, and Universitat de València for a grant within the program "Una Nau de Solidaritat". Support from the European Science Foundation (ESF) through COST Action P9 has been also obtained.

[1] C. E. Crespo-Hernández, B. Cohen, P. M. Hare, B. Kohler, *Chem. Rev.* **2004**, *104*, 1977.
[2] M. Daniels, W. W. Hauswirth, *Science* **1971**, *171*, 675.
[3] P. Vigny, M. Duquesne in *Organic Molecular Photophysics* (Ed.: J. B. Birks), Wiley, New York, **1977**, pp. 167–177.
[4] I. Jonas, J. Michl, *J. Am. Chem. Soc.* **1978**, *100*, 6834.
[5] J. P. Morgan, M. Daniels, *Chem. Phys. Lett.* **1979**, *67*, 533.
[6] P. R. Callis, *Chem. Phys. Lett.* **1979**, *61*, 563.
[7] P. R. Callis, *Ann. Pharm. Belg. Ann. Rev. Phys. Chem.* **1983**, *34*, 329.
[8] J. Peon, A. H. Zewail, *Chem. Phys. Lett.* **2001**, *348*, 255.
[9] E. Samoylova, H. Lippert, S. Ullrich, I. V. Hertel, W. Radloff, T. Schultz, *J. Am. Chem. Soc.* **2004**, *126*, 1782.
[10] C. Canuel, M. Mons, F. Pluzzi, B. Tardivel, I. Dimicoli, M. Elhanine, *J. Chem. Phys.* **2005**, *122*, 074316.
[11] T. Pancur, N. K. Schwalb, F. Renth, F. Temps, *J. Chem. Phys.* **2005**, *313*, 199.
[12] M. K. Kuimova, J. Dyer, M. W. George, D. C. Grills, J. M. Kelly, P. Matousek, A. W. Parker, X. Z. Sun, M. Towrie, A. M. Whelan, *Chem. Commun.* **2005**, 1182.
[13] A. L. Sobolewski, W. Domcke, *Chem. Phys.* **2000**, *259*, 181.
[14] a) J.-M. Percourt, J. Peon, B. Kohler, *J. Am. Chem. Soc.* **2000**, *122*, 9348; b) Erratum: J.-M. Percourt, J. Peon, B. Kohler, *J. Am. Chem. Soc.* **2001**, *123*, 5166.
[15] H. Kang, K. T. Lee, B. Jung, Y. Ko, S. K. Kim, *J. Am. Chem. Soc.* **2002**, *124*, 12958.
[16] N. Ismail, L. Blancafort, M. Olivucci, B. Kohler, M. A. Robb, *J. Am. Chem. Soc.* **2002**, *124*, 6818.
[17] M. Merchán, L. Serrano-Andrés, *J. Am. Chem. Soc.* **2003**, *125*, 8108.
[18] M. Merchán, L. Serrano-Andrés, M. A. Robb, L. Blancafort, *J. Am. Chem. Soc.* **2005**, *127*, 1820.
[19] R. J. Malone, A. M. Miller, B. Kohler, *Photochem. Photobiol.* **2003**, *77*, 158.
[20] S. Matsika, *J. Phys. Chem. A* **2004**, *108*, 7584.
[21] C. M. Marian, *J. Chem. Phys.* **2005**, *122*, 104314.
[22] S. Perun, A. L. Sobolewski, W. Domcke, *J. Am. Chem. Soc.* **2005**, *127*, 6257.
[23] L. Serrano-Andrés, M. Merchán, R. Lindh, *J. Chem. Phys.* **2005**, *122*, 104107.
[24] M. Klessinger, J. Michl, *Excited States and Photochemistry of Organic Molecules*, VCH Publishers, New York, **1995**.
[25] D. R. Yarkony in *Modern Electronic Structure Theory*, Part I (Ed.: D. R. Yarkony), World Scientific, Singapore, **1995**.
[26] M. A. Robb, M. Olivucci, F. Bernardi in *Encyclopedia of Computational Chemistry*(Eds.: P. von R. Schleyer, W. L. Jorgensen, H. F. Schaefer III, P. R. Schreiner, W. Thiel, R. Glen), Wiley, Chichester, **1998**.

[27] L. Serrano-Andrés, M. Merchán in *Encyclopedia of Computational Chemistry* (Eds.: P. von R. Schleyer, W. L. Jorgensen, H. F. Schaefer III, P. R. Schreiner, W. Thiel, R. Glen), Wiley, Chichester, **2004**.
[28] See books: a) *Conical Intersections* (Eds.: W. Domcke, D. R. Yarkony, H. Köppel), World Scientific, Singapore, **2004**; b) *Computational Photochemistry* (Ed.: M. Olivucci), Elsevier, Amsterdam, **2005**.
[29] T. Häupl, C. Windolph, T. Jochum, O. Brede, R. Hermann, *Chem. Phys. Lett.* **1997**, *280*, 520.
[30] A. Reuther, H. Iglev, R. Laenen, A. Laubereau, *Chem. Phys. Lett.* **2000**, *325*, 360.
[31] N. J. Kim, G. Jeong, Y. S. Kim, J. Sung, S. K. Kim, Y. D. Park, *J. Chem. Phys.* **2000**, *113*, 10051.
[32] D. C. Lührs, J. Viallon, I. Fischer, *Phys. Chem. Chem. Phys.* **2001**, *3*, 1827.
[33] E. Nir, C. Plutzer, K. Kleinermanns, M. De Vries, *Eur. Phys. J. D* **2002**, *20*, 317.
[34] C. Plützer, E. Nir, M. S. de Vries, K. Kleinermanns, *Phys. Chem. Chem. Phys.* **2001**, *3*, 5466.
[35] S. K. Mishra, M. K. Shukla, P. C. Mishra, *Spectrochim. Acta A*, **2000**, *56*, 1355.
[36] L. Serrano-Andrés. M. Merchán, I. Nebot-Gil, R. Lindh, B. O. Roos, *J. Chem. Phys.* **1993**, *98*, 3151.
[37] B. O. Roos, K. Andersson, M. P. Fülscher, P.-Å. Malmqvist, L. Serrano-Andrés, K. Pierloot, M. Merchán, *Adv. Chem. Phys.* **1996**, *93*, 219.
[38] M. Merchán, L. Serrano-Andrés, M. P. Fülscher, B. O. Roos in *Recent Advances in Multireference Methods* (Ed.: K. Hirao), World Scientific Publishing, Singapore, **1999**.
[39] R. González-Luque, M. Garavelli, F. Bernardi, M. Merchán, M. A. Robb, M. Olivucci, *Proc. Natl. Acad. Sci. USA* **2000**, *97*, 9379.
[40] M. Merchán, L. Serrano-Andrés in *Computational Photochemistry* (Ed.: M. Olivucci), Elsevier, Amsterdam, **2004**.
[41] J. M. Jean, K. B. Hall, *J. Phys. Chem. A*, **2000**, *104*, 1930.
[42] M. P. Fülscher, L. Serrano-Andrés, B. O. Roos, *J. Am. Chem. Soc.* **1997**, *119*, 6168.
[43] K. Andersson, M. Barysz, A. Bernhardsson, M. R. A. Blomberg, Y. Carissan, D. L. Cooper, M. Cossi, M. P. Fülscher, L. Gagliardi, C. de Graaf, B. Hess, G. Hagberg, G. Karlström, R. Lindh, P.-Å. Malmqvist, T. Nakajima, P. Neogrády, J. Olsen, J. Raab, B. O. Roos, U. Ryde, B. Schimmelpfennig, M. Schütz, L. Seijo, L. Serrano-Andrés, P. E. M. Siegbahn, J. Stålring, T. Thorsteinsson, V. Veryazov, P. -O. Widmark, MOLCAS, version 6.0, Department of Theoretical Chemistry, Chemical Centre, University of Lund, P.O.B. 124, S-221 00 Lund: Sweden, **2004**.
[44] S. J. Strickler, R. A. Berg, *J. Chem. Phys.* **1962**, *37*, 814.
[45] O. Rubio-Pons, L. Serrano-Andrés, M. Merchán, *J. Phys. Chem. A* **2001**, *105*, 9664.
[46] J. R. Platt, *J. Chem. Phys.* **1949**, *17*, 484.
[47] A. Broo, *J. Phys. Chem. A* **1998**, *102*, 526.
[48] A. L. Sobolewski, W. Domcke, *Eur. Phys. J. D* **2002**, *20*, 369.
[49] A. L. Sobolewski, W. Domcke, C. Dedonder-Lardeux, C. Jouvet, *Phys. Chem. Chem. Phys.* **2002**, *4*, 1093.
[50] S. Perun, A. L. Sobolewski, W. Domcke, *J. Chem. Phys.* **2005**, *313*, 107.
[51] J. Andreasson, A. Holmén, B. Albinsson, *J. Phys. Chem. B* **1999**, *103*, 9782.
[52] B. Albinsson, *J. Am. Chem. Soc.* **1997**, *22*, 113.
[53] N. J. Kim, H. Kang, Y. D. Park, S. K. Kim, *Phys. Chem. Chem. Phys.* **2004**, *6*, 2802.
[54] a) H. Kang, B. Jung, S. K. Kim, *J. Chem. Phys.* **2003**, *118*, 6717; b) Erratum: H. Kang, B. Jung, S. K. Kim, *J. Chem.Phys.* **2003**, *118*, 11336.
[55] S. Ullrich, T. Schultz, M. Z. Zgierski, A. Stolow, *J. Am. Chem. Soc.* **2004**, *126*, 2262.
[56] S. Ullrich, T. Schultz, M. Z. Zgierski, A. Stolow, *Phys. Chem. Chem. Phys.* **2004**, *6*, 2796.
[57] M. Zierhut, W. Roth, I. Fischer, *Phys. Chem. Chem. Phys.* **2004**, *6*, 5178.
[58] I. Hünig, C. Plützer, K. A. Seefeld, D. Löwenich, M. Nispel, K. Kleinermanns, *ChemPhysChem* **2004**, *5*, 1427.
[59] B. Cohen, P. M. Hare, B. Kohler, *J. Am. Chem. Soc.* **2003**, *125*, 13594.
[60] A. L. Sobolewski, W. Domcke, *Phys. Chem. Chem. Phys.* **2004**, *6*, 2763.
[61] T. Gustavsson, A. Sharonov, D. Onidas, D. Markovitsi, *Chem. Phys. Lett.* **2002**, *356*, 49.
[62] E. C. Lim in *Excited States, Vol. 3* (Ed.: E. C. Lim), Academic Press, New York, **1977**.
[63] W. A. Wassam Jr., E. C. Lim, *J. Chem. Phys.* **1978**, *68*, 433.
[64] E. C. Lim, *J. Phys. Chem.* **1986**, *90*, 6770.
[65] E. L. Rachofsky, J. B. A. Ross, M. Krauss, R. Osman, *J. Phys. Chem. A* **2001**, *105*, 190.
[66] B. Menucci, A. Toniolo, J. Tomasi, *J. Phys. Chem. A* **2001**, *105*, 4749.

Received: December 5, 2005
Revised: March 13, 2006
Published online: ■■ ▮▮, 2006

Computational Photophysics

L. Serrano-Andrés, M. Merchán, A. C. Borin* ..... ▮▮▮▮-▮▮▮▮

A Three-State Model for the Photophysics of Adenine

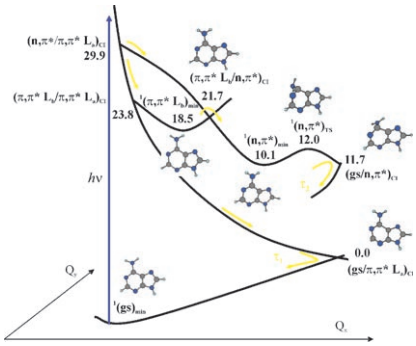

Multiple ultrafast deactivation of excited 9*H*- and 7*H*-adenine is explained on the basis of ab initio quantum-chemical CASPT2 calculations. The cornerstone of the quenched fluorescence of the system is efficient internal conversion through a barrierless pathway connecting the spectroscopic $^1(\pi\pi^* L_a)$ state with a funnel involving the ground state. Higher lying $^1(\pi\pi^* L_b)$ and $^1(n\pi^*)$ states are responsible for secondary and slower decays, as depicted in the scheme.